MARSH BULLETIN
EISSN 2957-9848

Marsh Bulletin Volume 21 Issue 1 (April 2026): 77-89

Synthesis and characterization of Clay /iron oxide nanocomposite and uses them to remove lead ions from aqueous solutions

Nadia khalaf Mohsen[1] Ahmed Yousif Hammood[1] and Muayad H. M. Albehadili[2]
[1]Department of Marine Environmental Chemistry, Marine Science Center, University of Basrah, Basrah, Iraq
[2] Department of Applied Marine Sciences, College of Education for Pure Science, University of Basrah, Iraq
E-mail: ahmed.hammood@uobasrah.edu.iq

Abstract
This study deals with the preparation of clay/iron oxide nanocomposite by co-precipitation method. Different techniques were used to characterize the prepared composite, such as FE-SEM, FT-IR, XRD, EDX, and Zeta Potential. XRD examinations revealed that the crystalline state of the composite was pure, while the particle size was 17.57 nm. In addition, the potential of the prepared nanocomposite as an adsorbent for lead was investigated. Four temperatures were used to study the adsorption isotherms and the Freundlich-Langmuir equation was applied. As a result, the Langmuir equation showed a stronger correlation than the Freundlich equation. The thermodynamic results of the study revealed that the adsorption process was spontaneous, as shown by the appearance of a negative value for (ΔG). The adsorption process was also endothermic, as the value of (ΔH) was positive, while the increased randomness was shown by the positive value of (ΔS). The practical application included the process of removing lead ions from samples in three locations: the first is Al-Faw (Ras Al-Bisha), the second is Shatt Al-Basra near the outlet of the main sewage station of the Basra Governorate Sewerage Directorate, and the third is Shatt Al-Basra (near the mangrove nursery) using a prepared absorbent surface. The removal rate was (93.87%) for the first location, (81.38%) for the second location, and (85.71%) for the third location.
Keywords: Adsorption; Clay/Iron oxide; Pb (II)ions, thermodynamic

Received 10 /9/ 2025 Accepted 23 /9/2025 Published 1 /4/2026

1.Introduction

Heavy metals are among the most dangerous environmental pollutants, as most of themare highly toxic and non-degradable, leading to their accumulation in ecosystems and increased concentrations over time. Water is one of the environmental media most vulnerable to the accumulation of metallic ions due to increased industrial activity, which raises significant environmental and health concerns, especially when these ions exceed environmentally permissible limits (Ali et al., 2019).

There are many sources of water pollution with heavy metals,with industrial activity being the primary source. These include waste from metallurgy, electroplating, tanning, battery manufacturing, dyes, and other industries. The danger of these ions lies in their cumulative and toxic effects on humans and animals, as they can enter the food chain and cause poisoning that may be

chronic and even carcinogenic in some cases (Igwe et al.,2005). Lead is known to be unnecessary for biological processes and is classified as a highly toxic element, even at low concentrations. Studies indicate that lead contamination of soil may result in inhibition of microbial biomass (Nagajyoti et al., 2010) and exposure to it can cause damage to the spleen, liver, and blood, in addition to its association with certain types of cancer (Hosseini et al.,2020; Yu, Wang and Zhang, 2014) Given these risks, the removal of heavy metals from contaminated water has become a major focus of scientific research. Several techniques have been developed to treat these contaminants, including chemical precipitation process (Omidi et al.,2019) adsorption (Namasivayam and Sangeetha,2002), ion exchange method (Verbych et al.,2004) treatment using electrochemical method (Tran et al.,2017) and membrane filtration (Sudilovskiy et al.,2007) among others. Research indicates that combining these techniques can enhance removal efficiency (Bazrafshan et al.,2017) (Blöcher et al.,2003) Among these techniques, adsorption is a promising and effective method, due to its low cost and ease of application, and the possibility of using multiple natural materials as adsorbents. Among these materials, clay is of particular interest due to its abundant resources and diverse chemical and physical properties. Clay is a natural resource of great importance in many industrial, agricultural, and environmental fields, due to its unique chemical and physical composition. Clay is predominantly composed of hydrated aluminum silicates, with additional minerals such as quartz, iron, and magnesium, as well as organic compounds and dissolved salts. This composition gives it exceptional properties, including high adsorption capacity and ion exchange capacity, making it widely applicable in many sectors (Habboush,1983). Among clay minerals, bentonite is one of the most important. It is composed primarily of crystalline clay minerals belonging to the montmorillonite group, whose chemical formula is (Al_2O_3•4SiO_2•H_2O). (British PharmaCopoeia ,1993) Regarding the preparation method, the co-precipitation technique is one of the effective methods for preparing nanoparticles. This technique relies on the reaction of metal in an alkaline medium. The addition of bases, such as ammonium hydroxide, leads to the gradual precipitation of metal ions, which contributes to a reduction in the crystal growth rate and leads to the formation of stable nanoparticles with a homogeneous size distribution This technology is an economical and environmentally friendly alternative to conventional techniques. (Salway,2006). The current study focused on applying the adsorption phenomenon to remove a common toxic element, lead, from aqueous solutions. It aims to use the prepared compound as an adsorbent surface to verify its efficiency in adsorbing lead ions from contaminated water, contributing to the provision of effective solutions for treating this type of pollution.

2. Materials and Methods

2.1. Nano-clay preparation method

Natural clay was collected from the sediments of the Arabian Gulf in the Ras Al-Bishaarea.Basrah-Iraq. After collection, the clay was manually cleaned and dried, then ground for (30min) using a nanoball mill. A weight(50g) sample of the ground clay was treated with a 10% hydrogen peroxide (H_2O_2) solution at (30°C) for (20min) to remove organic carbon. The powder was then washed with water containing hydrochloric acid (HCl) to adjust the pH to 4, under continuous agitation at (800rpm) for (30min) to remove inorganic carbon. The suspension was allowed to settle for (3h), and the filtrate with suspended impurities was removed, leaving the stabilized nanoclay. The remaining

precipitate was transferred to a (500ml) beaker and dried at (105°C) for (12h). After that, it was ground again using a ball mill for (5h), and then subjected to a firing process at (720°C) for (6h) **(**Tarekegn et al.,2023)**.**

2.2. Nano-iron oxide coating with nanoclay

The co-precipitation method was used to prepare the material. (0.375g) of iron sulfate ($FeSO_4$) was dissolved in (50ml) and (0.75g) of iron nitrate ($Fe(NO_3)_3.9H_2O$) was dissolved in (0.5ml) of deionized water. One gram of nanoclay was dissolved in (20ml) of deionized water with continuous stirring for (15min). After complete dissolution, the three solutions were mixed in a three-necked flask with a continuous flow of nitrogen gas. The temperature of the mixture was increased to (80°C). (30ml) of ammonium hydroxide (NH_4OH) was then added in (10ml/min) increments with stirring. The solution was then stirred for (1h) and allowed to cool to room temperature. The precipitate was washed several times with deionized water until the pH was neutral. The precipitate was then washed once with ethanol, and then with deionized water for a final time. The precipitate was separated with a magnet and dried at (60°C) for (6h). The precipitate was then finely crushed.

3.2. Characterization Techniques

The prepared compound was characterized using several advanced international techniques. These included X-ray diffraction spectroscopy (XRD) (PANalytical, UK), FTIR (Shimazu, Japan), zeta potential (Malvern, Japan), scanning electron microscopy (FESEM) (TE SCAN, Czech Republic), and energy dispersive X-ray (TE SCAN, Czech Republic). Lead concentrations were determined using flame atomic absorption spectroscopy (AA500Pg instruments, UK).

4.2. Adsorption studies

A standard lead solution of (1000 mg. L^{-1}) was prepared by dissolving 1.598 g of Pb $(NO_3)_2.4H_2O$ in (1L) of distilled water. A range of concentrations was then prepared that matched the sensitivity of the FAAS used, and these concentrations ranged between (125-200 mg. L^{-1}). The pH range of (3-9) Buffer solutions were used to cover an appropriate PH range in order to determine the optimum, the time required to reach equilibrium on the prepared nanocomposite surface was studied over different time period, in the range of (5–180min) , at a temperature of (25°C). andthe initial volume and concentration of thePb (II) ion were (150mg.L^{-1}, 25mL), Using a weight of the nanocomposite (0.02 g), the vials were then placed in a shaking incubator at a speed of (120 rpm). The absorption capacity (Qe) and the absorption percentage (R%) were calculated using equations 1 and 2 (Jain et al.,2019)**.**

$Q_e = V(C_o - C_e)/m$ …… (1)

Removal ratio $= [(C_o - C_e)/C_o] \times 100$ ……. (2)

Where; Qe represents the adsorption capacity (mg/g), V is the volume of the solution (L), m represents the weight of the adsorbent (g), Ce represents the concentration of the remaining adsorbent in (mg/L-1), Co is the initial concentration of the adsorbent in (mg/L), and Ce represents the concentration of the remaining adsorbent in (mg/L-1).

5.2. Thermodynamic Parameters

concentrations of pb (II) ions were prepared (125-200 mg. L^{-1}). The Samples were then placed in vials, to which (0.02g) of coatednanoclay with nanoiron was added. The vials were shaken at (120 rpm) for the required time at various temperatures: (10.0, 25.0, 37.5, and50.0°C). After centrifugation, the remaining lead concentrations were measured. The thermodynamic functions, enthalpy (ΔH), entropy (ΔS), and free energy (ΔG), were determined using Equations (3-5).

$\Delta G = -RT \ln k$……. (3)

$K = C_{solid} / C_{liqui.d}$ ..... (4)

$\ln K = \Delta S / R - \Delta H / RT$... (5)

Where K is the equilibrium constant, Cliquid is the equilibrium liquid phase concentration (mg/L), Csolid is the equilibrium solid phase concentration (mg/L), ΔG represents the Gibbs free energy (kJ mol-1), R represents the gas constant (0.0083 kJ K mol-1), ΔH (kJ mol-1) and ΔS (kJ mol-1) were calculated by the slope using Equation (5**)** (Ge and Ma,2015).

6.2. Method activates adsorbent surface

To reuse and activate the adsorbent, lead ions were recovered by weighing 0.02 g of the adsorbent and adding a volume of 25 ml with a concentration of 150 mg/L of lead ions. The samples were shaken for a suitable equilibrium time of 60 min at 25°C and a speed of 120 rpm. A magnetic field was then used to remove the adsorbent. Hydrochloric acid with a concentration of 0.5 N and a volume of 25 ml was added to the remaining adsorbent. The conical flasks were shaken for 60 min. The adsorbent was then removed from the filtrate by an external magnet, and the concentration of the recovered lead ions was estimated (Theurer,2019). Equation (6) was used to calculate the recovery ratio (S%) (Soldatkina and Zavrichko, 2019).

$$S\% = \frac{C_d \ V_d}{Q_e \ m} \times 100 \quad \ldots\ldots\ldots\ldots (6)$$

Where: - S% represents the percentage of recovery, Cd represents the concentration of the solution after the adsorption process (mg/L), Qe represents the weight capacity of adsorption (mg/g), m represents the weight of the nanomaterial (g), and Vd represents the volume of the washing solution (L).

3.Results and discussion:

Figure (1.a) shows the infrared spectra of the nanoclay-coated with nano -iron, showing distinct absorption bands in the range (922.83-1151.23cm^{-1}) attributed to the Si-O bond, indicating the continuity of the silicate structure after the coating process. A multi-band absorption band also appeared in the range (480.30 - 779.71 cm^{-1}) indicating absorption of the Al-O group as well as the M-O (oxygen-metal) groups, which represent bonds between oxygen and various metal elements, including the Fe-O bond (Silverstein, Webster and Kiemle, 2005).

Figure 1**.** (b) shows the X-ray diffraction pattern of the prepared compound. The results showed a clear diffraction peak within the angular range (80-10=2Ɵ) at the following location

2Ɵ = (20.85), (26.80), (26.87), (29.68), (33.28), (39.69), (50.35), (60.30), with the highest intensity peak at (θ2° = 26.80). The peaks at (26.89), (26.95), (29.68), and (50.35) indicate the presence of quartz, while the peak at (20.85) is due to montmorillonite. The two peaks at (33.28), (39.85) indicate the presence of montmorillonite in addition to magnesium and calcium, while the peak at (60.30) indicates the presence of iron. These results are consistent with the work of the researcher (Saleh) and his group (Saleh,1980) and the researcher (Tarekegn) and his group (Tarekegn et al., 2020). The crystallite sizes of the prepared compounds were calculated using the Debye-Scherrer equation (Monshi,Foroughi and Monshi ,2012).shown in (2), based on the width of the peak at mid-intensity (FWHM) of the highest peak in the X-ray diffraction spectrum. The results showed that the prepared compounds possess crystallite sizes purity and the partical size of 17.57 nm

D=Kλ/(β_hklCOSθ) …….... (7)

Where:

D: crystallite size (nm).

K: shape factor, with a value of approximately (0.90-0.94).

λ: The wavelength of Cu-K-alpha radiation, equal to 1.5406 Å (equivalent to 0.154 nm).

βhkl: The full width at half maximum (FWHM) of the peak, in units of radial angles. Convert values given in degrees to radial angles by first dividing θ2 by 2, then multiplying by 0.01745 to convert to radial angles.

θ: The angle of incidence of the X-rays, in units of radial angles

Figures 1. (c) represent FE-SEM images of thenanoclay-coated composite, which showed quasi-spherical particle patterns. The images also showed clear agglomerations in the surface structure, in addition to the presence of pores or holes on the surfaceof the composite.Microscopic image analysis results indicate that the prepared composite possesses crystal sizes in the nanoscale range. To accurately determine the particle dimensions, Image-J software, a proven image analysis and particle size measurement tool, was used. The analysis results showed removing contaminants from aqueous solutions and treating industrial water

Figures 1. (d) Energy-dispersive X-ray (EDX) spectrum of the nanoclay-coated with nanoironcomposite. The energy-dispersive X-ray (EDX) spectrum of the clay-coated composite, shows three energy peaks at 0.7 keV, 6.4 keV, and 7.1 keV, attributed to iron. One of these peaks was strongly and distinctly expressed, while the other two peaks were less intense. An energy peak at 0.52 keV was also recorded, attributed to oxygen. In addition, a group of other peaks appeared, attributed to carbon, nitrogen, calcium, magnesium, aluminum, silica, and potassium, in addition to the iron and oxygen peaks, reflecting the diverse composition of the nanoclay used in the preparation of the composite

that the average particle dimensions reflect the structural composition of the composite.In the case of the coated clay, the granular characteristics were accurately determined, with particle sizes ranging from 5.319 µm to 31.914 µm, with an average of 19.577 µm. This granular distribution reflects the material's moderate to high specific surface area, which enhances its adsorption efficiency.The smaller the particle size, the greater the surface area available for ions or molecules to interact with surface active sites, making the coated clay an effective material for

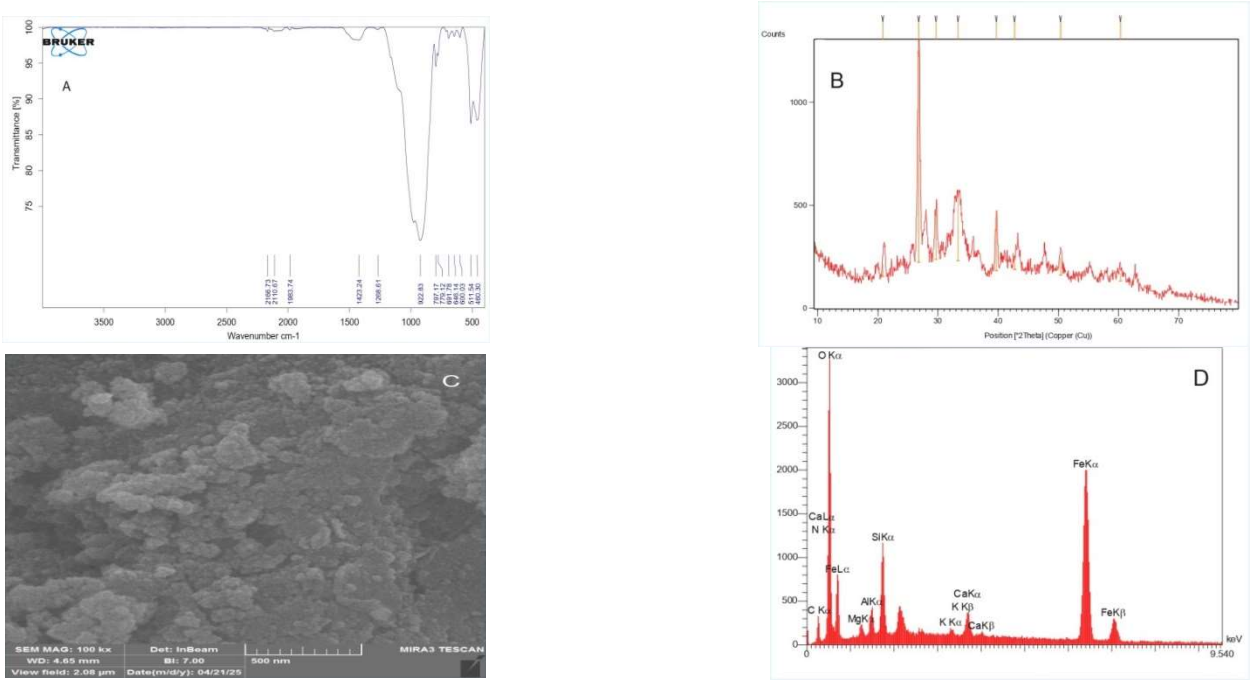

Figure. 1. (a) FTIR spectra, (b) XRD, (c) FESEM and (d) EDX of nano–coated clay

6.3 Zeta potential

The zeta potential provides important information about the stability and charge of colloidal particles, as particles with similar charges are affected by electrostatic attraction, causing them to separate and move apart. Zeta potential values greater than ±30 mV indicate excellent physical stability of colloidal materials, while values less than ±30 mV indicate physical instability of colloidal particles. (Honary and Zahir, 2013). The zeta potential value of a nanoclay composite coated with nanoiron was determined, and the results showed a value of (-33.9 mV). This means that the particles are stable in their aqueous solutions, as shown in Figure (2)) Al-Graiti,Al-Dokheily and Magtoof, 2022 ; Mohammed et al., 2021).

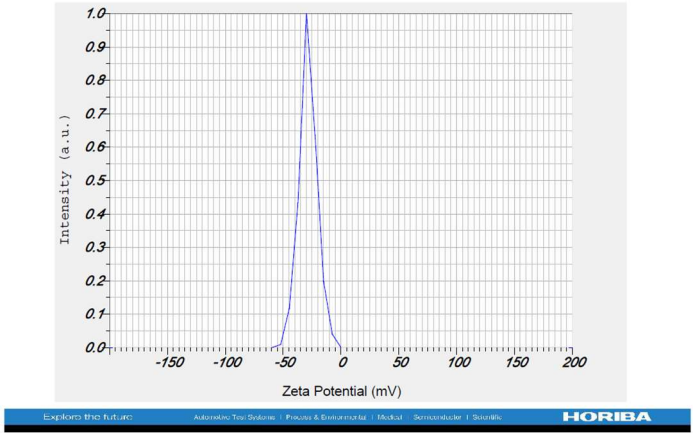

Figure. 2. Zeta potential

4.Adsorption studies

4.1. Effect of contact time

A range of (5-180 min) was used to determine the contact time for lead adsorption at a temperature of (25°C). According to the results of the study shown in Figure (3), the contact time was (60 min), where the percentage of removal was (90.94%). The figure also showed a significant increase in the first minutes of the adsorption process on the adsorbent surface, after which there appeared a slowdown until reaching the contact time and saturation of the active sites of the adsorbent surface (Saleh, 1980; Elhussien and Isa, 2015).

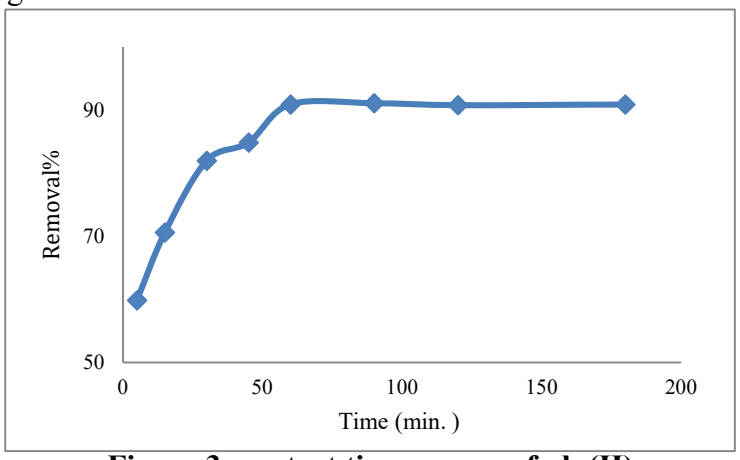

Figure.3. contact time curves of pb (II)

4.2. Effect of pH

The adsorption process is affected by either an increase or a decrease when changing the value of the hydrogen number of aqueous solutions, as it affects the nature of the adsorbent material, and may also affec
the solubility of the adsorbed material (Adamson and Gast, 2001) The effects of pH on the adsorption of Pb (II) ion onto nanoclay composite coated with nanoiron were studied at different pH values (3, 5, 7, and 9) using a fixed concentration and a (60min) contact time of Pb (II) at (25°C).

According to the results shown in Figure (4), there is a clear increase in the lead adsorption rate as the solution's alkalinity increases. In acidic media, the active sites acquire a positive charge, causing repulsion between lead ions and the adsorbent surface. When the pH increases, the active sites begin to deproteinize, allowing lead ions to bind. Also, increasing the pH causes a decrease in the solubility of lead ions in the solution, which leads to the lead ions converging with the adsorbent surface (Hammood, Mohammed and Majeed,2023) (Lund, 1994) To avoid interference between the adsorption process and the precipitation process, (pH 5) was used to study the remaining factors.

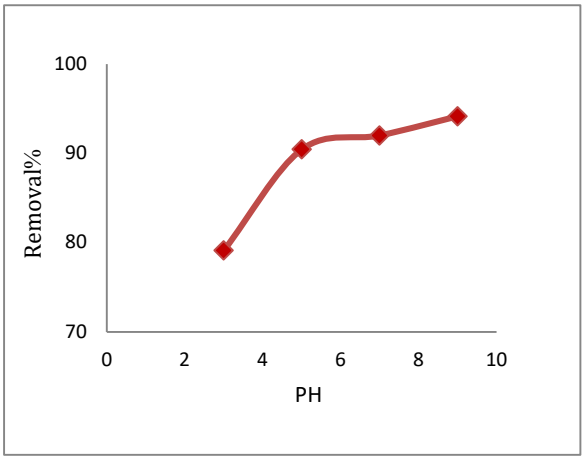

Figure 4. Effect of pH

4.3. Adsorption isotherm

Four temperatures within the range (10, 25, 37, and 50°C) were used to study the adsorption isotherms. Figure (5) shows a plot of the concentration at equilibrium (Ce) with the adsorption capacity (Qe).

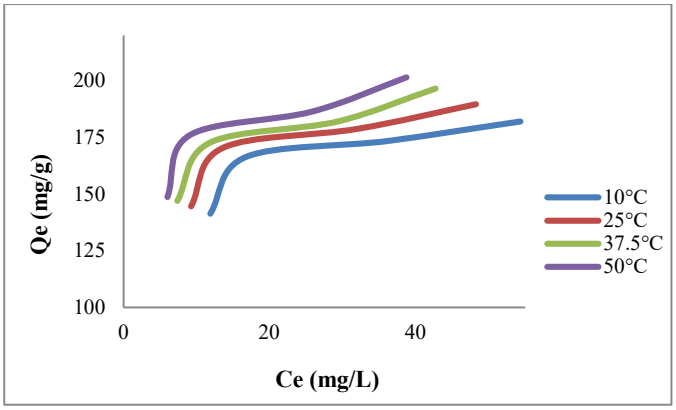

Figure. 5 .Adsorption isotherm

Figure (5) shows that the general form of the isothermal adsorption of lead ions using four temperatures is consistent with type (H), according to Giles' classificationThis type isotherm is based on the Langmuir principle. and indicates a high adsorbtion affinity, as it appears even in very dilute solutions this isotherm is observed even in very dilute solutionsit is observed that the amountofPb(II) ions adsorbed onto the studied surface increases with the initial lead concentration. This increase is attributed to enhanced electrostatic interactions between solutions on the surface under study. The Freundlich

-Walkemuir equation (8,9) was used to study the nature of adsorption (Wang, Zhuang, Peng, and Li, 2006). Table (1) displays the adsorption data for the isothermal adsorption line:

logQe = logKf + 1/n logCe. . .... (8) Ce/Qe = 1/Qmb + Ce/Qm . . .. (9)

where n represents the adsorption intensity, Kf is the adsorption capacity, b is the adsorption energy, and Qm is the maximum adsorption capacity (mg/g).

the Pb(II) ions and the active sites on the adsorbent surfaces (Atkins, De Paula, and Keeler, 2023)(Kapoor ,1994) moreover, the amount of adsorbed ions increases with temperature suggesting that the process,which indicates the endothermic nature of the adsorption process is (endothermicand that higher temperature enhance the adsorption efficiency.to futher describe the adsorbtion mechanism, The Langemuir-Freundlich model was applied to the adsorption of lead from their aqueous

The results, as shown in Table (1), showed that the values of the correlation coefficient (R^2) for the Langmuir equation are higher than the values of the Freundlich equation, which indicates that the adsorption process occurred on a homogeneous surface. Also, the adsorption process was single-layer, which also indicates that the surface contains sites with equal energy (Al-Saadie and Jassim, 2010*)*

Table1. Results Freundlich and Langmuir isotherms

Temp. (C)	Langmuir constants			Freundlich constants		
	Q_m (mg/g)	b (L/mg)	R^2	n	Kf	R^2
10.0	194.060	0.272	0.9988	7.022	104.335	0.8128
25.0	201.240	0.308	0.9984	7.073	110.483	0.8476
37.5	207.253	0.342	0.9975	6.967	114.421	0.8891
50.0	211.282	0.420	0.9978	7.253	121.483	0.8644

4.4 The study of thermodynamics

Four temperatures within the range (10-50°C) were used to study the thermodynamics functions (ΔG, ΔH, and ΔS) as shown in Table (2).

Table 2. Thermodynamic functions

Co (mg/L)	K				- ΔG				ΔH	ΔS
	Temperature									
	283	298	310.5	323	283	298	310.5	323		
125	9.53	12.51	15.93	19.76	-51.98	-62.00	-70.36	-78.71	137.11	0.66
150	7.91	10.00	11.67	15.46	-47.45	-56.40	-63.86	-71.32	121.43	0.59
175	3.83	4.46	4.97	5.77	-30.96	-36.59	-41.28	-45.97	75.18	0.37
200	2.67	3.14	3.68	4.16	-22.64	-28.26	-32.94	-37.63	83.39	0.37

Figure (6) shows the relationship between 1/T and lnK where the correlation coefficient was in the range (R≥ 0.9983-0.9963). Table (2) shows through the positive values of (ΔH) that the adsorption reaction is of the endothermic type (Hefne et al., 2008) where the enthalpy values ranged between (75.18 and 137.11 kJ/mol-1).

The values of (ΔS) were positive, indicating increased randomness (Lafi and Hafiane, 2015). The values of (ΔG) were all negative, indicating that the adsorption process occurred spontaneously. (Cheng et al., 2014) as their values ranged between (-22.64) and (78.71) kJ mol-1. From these values, it is clear that the type of adsorption was physical, as the literature indicates that when the values of (ΔG) range from (0) to (-20) kJ mol-1, then the adsorption is physical(Vakili, et al., 2019)

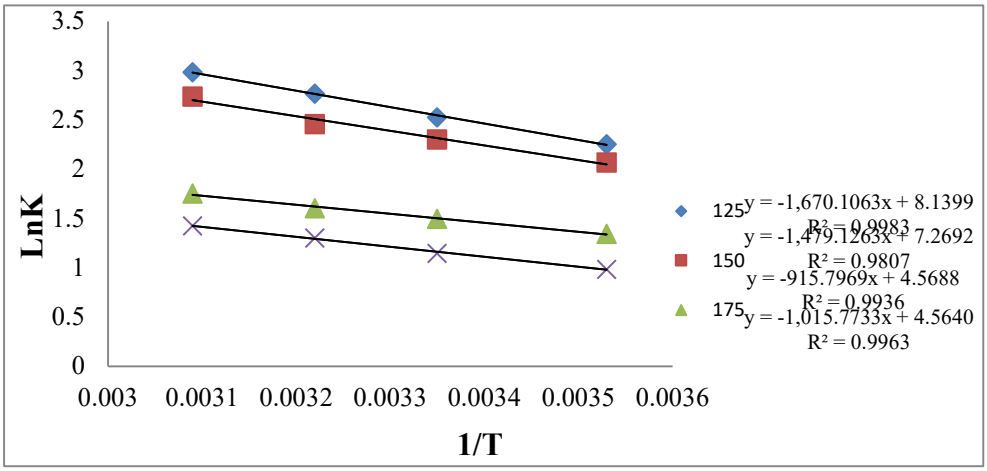

Figure. 6. Plot of lnK against 1/T for adsorption

4.5. Practical applications

The practical applications involved the use of the prepared adsorbent surface to remove lead ions from seawater and wastewater samples taken from three different sites: the first site in Al-Faw (Ras Al-Bisha); the second site on the Shatt Al-Basra River near the wastewater outlet of the Hamdan Main Station affiliated with the Basra Governorate Sewerage Directorate; and the third site on the Shatt Al-Basra River near the mangrove nursery.The results, as shown in Table (3), demonstrated the high effectiveness of the prepared adsorbent surfaces in removing lead ions, as the removal percentage was (93.87%) for the first siteand for second site was (81.38%)and third site was (85.71).These results indicate the potential of these surfaces as effective materials for treating water contaminated with lead ions.

Table 3: Practical applications for removing lead

Site	Contact time (min)	pH	Co (mg/L)	C_e (mg/L)	Removal%	Q_e (mg/g)
St1	60	8.51	0.147	0.009	93.87	0.1725
St2	60	7.72	0.231	0.043	81.38	0.235
St3	60	8.35	0.077	0.011	85.71	0.0825

4.6. Activate adsorbent surfaces

The recovery Pb (II) ions from the surfaces of the prepared adsorbents was studied, given its importance in the possibility of reusing these surfaces and recovering the adsorbed ions from them. showed that the recovery rate in the first activation process was high, reaching (95.35%) . However, a decrease in the recovery rate was observed during the second activation process, reaching92(.41%) . These results indicate that the prepared adsorbent can be reused multiple times while maintaining its efficiency in adsorbing lead ions. The dissociation of Pb^{2+} ions in an acidic medium is attributed to the increased concentration of hydrogen ions (H+) at low pH, which leads to competition between them and lead ions for active sites on the surface of the adsorbent, thus reducing adsorption and increasing the dissociation rate.

5.Conclusion

In this study, iron-coated nanoclay particles were produced using a chemical co-precipitation technique to investigate the potential of the prepared surface as an adsorbent for lead removal. The effects of variables that may affect the adsorption process, such as pH, contact time, initial element concentration, and temperature, were studied. The contact time was 60 min. The effects of pH levels between 3 and 9 were also studied. According to the study, 90.94% of lead ions were removed. The isothermal adsorption was calculated using the Langmuir and Freundlich models, and the Langmuir model was found to be more suitable for adsorption than the Freundlich model. Based on the results, the resulting compound can be used as a lead adsorbent and is believed to have important applications in environmental protection, as the adsorption reaction was spontaneous and endothermic according to thermodynamic criteria. This study presents practical applications for the removal of lead ions from marine water samples collected from threedifferent sites: the first site in Al-Faw (Ras Al-Bisha); the second site on the Shatt Al-Basra River near the wastewater outlet of the Hamdan Main Station affiliated with the Basra Governorate Sewerage Directorate; and the third
site on the Shatt Al-Basra River near the mangrove nursery. The results, as shown in Table (3), demonstrated the high effectiveness of the prepared adsorbent surfaces in removing Pb (II) ions.

References

Adamson, A. W., & Gast, A. P. (2001). *Physical chemistry of surfaces* (6th ed.). John Wiley and Sons.

Ali, H., Khan, E., & Ilahi, I. (2019). Environmental chemistry and ecotoxicology of hazardous heavy metals: Environmental persistence, toxicity, and bioaccumulation. *Journal of Chemistry, 2019,* 6730305. https://doi.org/10.1155/2019/6730305

Al-Graiti, W., Al-Dokheily, M., & Magtoof, M. S. (2022). Synthesis and characterization of nanosized iron using three different methods. *Journal of College of Education for Pure Sciences, 12*(1), 8–15.

Al-Saadie, K. A., & Jassim, S. B. (2010). Adsorption study for chromium (VI) on Iraqi bentonite. *Baghdad Science Journal, 7*(1), 745–756. https://doi.org/10.21123/bsj.2010.7.1.745-756

Atkins, P. W., De Paula, J., & Keeler, J. (2023). *Atkins' physical chemistry.* Oxford University Press.

Bazrafshan, E., Sobhanikia, M., Mostafapour, F. K., Kamani, H., & Balarak, D. (2017). Chromium biosorption from aqueous environments

by mucilaginous seeds of *Cydonia oblonga*: Kinetic and thermodynamic studies. *Global NEST Journal, 19*(2), 269–277. https://doi.org/10.30955/gnj.001708

Blöcher, C., Dorda, J., Mavrov, V., Chmiel, H., Lazaridis, N. K., & Matis, K. A. (2003). Hybrid flotation-membrane filtration process for the removal of heavy metal ions from wastewater. *Water Research, 37*(16), 4018–4026. https://doi.org/10.1016/S0043-1354(03)00314-2

British Pharmacopoeia. (1993). *British pharmacopoeia* (30th ed., pp. 58, 147, 231, 371). HMSO, London.

Cheng, C., Liu, Z., Li, X., Su, B., Zhou, T., & Zhao, C. (2014). Graphene oxide interpenetrated polymeric composite hydrogels as highly effective adsorbents for water treatment. *RSC Advances, 4*(80), 42346–42357. https://doi.org/10.1039/C4RA07114J

Elhussien, M. H., & Isa, Y. M. (2015). Acetic acid adsorption onto activated carbon derived from pods of *Acacia nilotica var. astringens* (sunt tree) by chemical activation with $ZnCl_2$. *Journal of Natural Sciences Research, 5*(10). https://doi.org/10.51415/10321/3022

Ge, H., & Ma, Z. (2015). Microwave preparation of triethylenetetramine modified graphene oxide/chitosan composite for adsorption of Cr(VI). *Carbohydrate Polymers, 131,* 280–287. https://doi.org/10.1016/j.carbpol.2015.06.025

Habboush, A. E. (1983). *Separation methods in chemical analysis.* Mosul University Press.

Hefne, J. A., Mekhemer, W. K., Alandis, N. M., Aldayel, O. A., & Alajyan, T. (2010). Kinetic and thermodynamic study of the adsorption of Pb(II) from aqueous solution to the natural and treated bentonite. *International Journal of Physical Sciences.* https://doi.org/10.5897/IJPS.9000337

Hammood, A. Y., Mohammed, I. K., & Majeed, A. A. (2023). Removal of Cd(II) ions from aqueous solutions using adsorption by bentonite clay and study of the adsorption thermodynamics. *Pollution, 9*(4), 994–1005. https://doi.org/10.22059/poll.2023.353137.1741

Honary, S., & Zahir, F. (2013). Effect of zeta potential on the properties of nano-drug delivery systems – A review (Part 1). *Tropical Journal of Pharmaceutical Research, 12*(2), 255–264. https://doi.org/10.4314/tjpr.v12i2.19

Hosseini, N. S., Sobhanardakani, S., Cheraghi, M., et al. (2020). Heavy metal concentrations in roadside plants (*Achillea wilhelmsii* and *Cardaria draba*) and soils along some highways in Hamedan, west of Iran. *Environmental Science and Pollution Research, 27*(12), 13301–13314. https://doi.org/10.1007/s11356-020-07874-6

Igwe, J. C., Nwokennaya, E. C., & Abia, A. A. (2005). The role of pH in heavy metal detoxification by bio-sorption from aqueous solutions containing chelating agents. *African Journal of Biotechnology, 4*(10), 1109–1112. http://dx.doi.org/10.4067/S0717-34582007000400007

Jain, P., Kaur, M., & Kaur, M. (2019). Comparative studies on spinal ferrite (M = Mg/Co) nanoparticles as potential adsorbents for Pb(II) ions. *Bulletin of Materials Science, 42,* 77. https://doi.org/10.1007/s12034-019-1743-2

Kapoor, K. L. (1994). *A textbook of physical chemistry.* Macmillan India Limited.

Lafi, R., & Hafiane, A. (2015). Removal of methyl orange (MO) from aqueous solution using cationic surfactants modified coffee waste (MCWs). *Journal*

of the Taiwan Institute of Chemical Engineers, 58, 424–433. https://doi.org/10.1177/0263617418819227

Lund, W. (1994). *The pharmaceutical codex* (12th ed., pp. 774–8512). Pharmaceutical Press. ISBN: 9780853692904

Mohammed, I., Al Shehri, D., Mahmoud, M., Kamal, M. S., & Alade, O. S. (2021). Impact of iron minerals in promoting wettability alterations in reservoir formations. *ACS Omega, 6*(5), 4022–4033. https://doi.org/10.1021/acsomega.0c05954

Monshi, A., Foroughi, M. R., & Monshi, M. R. (2012). Modified Scherrer equation to estimate more accurately nano-crystallite size using XRD. *World Journal of Nano Science and Engineering, 2*(3), 154–160. https://doi.org/10.4236/wjnse.2012.23020

Nagajyoti, P. C., Lee, K. D., & Sreekanth, T. V. M. (2010). Heavy metals, occurrence and toxicity for plants: A review. *Environmental Chemistry Letters, 8*(3), 199–216. https://doi.org/10.1007/s10311-010-0297-8

Namasivayam, C., & Sangeetha, D. (2002). Removal of Congo Red from water by adsorption onto activated carbon prepared from coir pith, an agricultural solid waste. *Dyes and Pigments, 54*(1), 47–58. https://doi.org/10.1016/S0143-7208(02)00025-6

Omidi, A. H., Cheraghi, M., Lorestani, B., et al. (2019). Biochar obtained from cinnamon and cannabis as effective adsorbents for removal of lead ions from water. *Environmental Science and Pollution Research, 26,* 27905–27914. https://doi.org/10.1007/s11356-019-05997-z

Salway, J. G. (2006). *Biochemistry at a glance* (2nd ed.). Blackwell Publishing.

Saleh, J. M. (1980). *Surface chemistry* (1st ed.). Baghdad University Press.

Silverstein, R. M., Webster, F. X., & Kiemle, D. J. (2005). *Spectrometric identification of organic compounds* (7th ed., p. 512). Wiley.

Soldatkina, L., & Zavrichko, M. (2019). Equilibrium, kinetic, and thermodynamic studies of anionic dyes adsorption on corn stalks modified by cetylpyridinium bromide. *Colloids and Interfaces, 3*(1), 4. https://doi.org/10.3390/colloids3010004

Sudilovskiy, P. S., Kagramanov, G. G., Trushin, A. M., & Kolesnikov, V. A. (2007). Use of membranes for heavy metal cationic wastewater treatment: Flotation and membrane filtration. *Clean Technologies and Environmental Policy, 9,* 189–198. https://doi.org/10.1007/s10098-007-0086-7

Tarekegn, M. M., Balakrishnan, R. M., Hiruy, A. M., Dekebo, A. H., & Maanyam, H. S. (2023). Nano-clay and iron impregnated clay nanocomposite for Cu^{2+} and Pb^{2+} ions removal from aqueous solutions. *Environmental Nanotechnology, Monitoring & Management, 20,* 100763. https://doi.org/10.1177/11786221221094037

Tarekegn, M. M., Balakrishnan, R. M., Hiruy, A. M., Dekebo, A., & Hussen, A. (2020). Nano-clay and iron impregnated clay nanocomposite for Cu^{2+} and Pb^{2+} ions removal from aqueous solutions. *International Journal of Environmental Analytical Chemistry, 100*(1), 1–16. http://dx.doi.org/10.1177/1178622122109 4037

Theurer, J. (2019). *Removal of residual oil from produced water using magnetic nanoparticles* (Master's thesis). University of Oklahoma, USA.

Tran, T. K., Leu, H.-J., Chiu, K.-F., & Lin, C.-Y. (2017). Electrochemical treatment of heavy metal-containing wastewater with the removal of COD and heavy metal

ions. *Journal of the Chinese Chemical Society, 64*(5), 493–502. https://doi.org/10.1002/jccs.201600266

Vakili, M., et al. (2019). Regeneration of chitosan-based adsorbents used in heavy metal adsorption: A review. *Separation and Purification Technology, 224,* 373–387. https://doi.org/10.1016/j.seppur.2019.05.040

Verbych, S., Hilal, N., Sorokin, G., & Leaper, M. (2004). Ion exchange extraction of heavy metal ions from wastewater. *Separation Science and Technology, 39*(9), 2031–2040. https://doi.org/10.1081/SS-120039317

Wang, X., Zhuang, J., Peng, Q., & Li, Y. (2006). Hydrothermal synthesis of rare-earth fluoride nanocrystals. *Inorganic Chemistry, 45*(17), 6661–6665. https://doi.org/10.1021/ic051683s

Yu, X. Z., Wang, D. Q., & Zhang, X. H. (2014). Chelator-induced phytoextraction of zinc and copper by rice seedlings. *Ecotoxicology, 23,* 749–756. https://doi.org/10.1007/s10646-014-1188-8

تحضير وتشخيص مركب نانوي من الطين وأكسيد الحديد واستخدامه لإزالة أيونات الرصاص من المحاليل المائية

نادية خلف محسن، احمد يوسف حمود، مؤيد حسن محمد

المستخلص

تتناول هذه الدراسة تحضير مركب نانوي من الطين وأكسيد الحديد بطريقة الترسيب المشترك. استُخدمت تقنيات مختلفة لتشخيص المركب المُحضر، مثل المجهر الالكتروني الماسح (FE-SEM)، ومطياف الأشعة تحت الحمراء(FT-IR) ، وتقنية حيود الأشعة السينية(XRD) ، وتقنيةEDX ، وجهد زيتا. أظهرت فحوصات حيود الأشعة السينية (XRD) أن الحالة البلورية للمركب نقية، بينما بلغ حجم الجسيمات 17.57 نانومتر. كما تم دراسة إمكانية استخدام المركب النانوي المُحضر كمادة مازة لعنصر الرصاص. استُخدمت أربع درجات حرارة لدراسة ايزوثيرمات الامتزاز، وطُبقت معادلة فروندليش ولانكماير. ونتيجةً لذلك، أظهرت معادلة لانكماير ارتباطًا أقوى من معادلة فروندليش. أظهرت النتائج الديناميكية الحرارية للدراسة أن عملية الامتزاز تلقائية، كما يتضح من ظهور قيمة سالبة لـ (ΔG) وكانت عملية الامتزاز ماصة للحرارة أيضًا، حيث كانت قيمة (ΔH) موجبة، بينما أظهرت القيمة الموجبة لـ (ΔS) زيادة في العشوائية. تضمن التطبيق العملي عملية إزالة أيونات الرصاص عينات مياه بحرية من ثلاث مواقع: الأول هو الفاو (رأس البيشة)، والثاني هو شط البصرة بالقرب من مخرج محطة الصرف الصحي الرئيسية لمديرية مجاري محافظة البصرة، والثالث هو خور الزبير (بالقرب من مشتل المنجروف) باستخدام السطح الماز المحضر. بلغت نسبة الإزالة (93.87%) للموقع الأول، و(81.38%) للموقع الثاني، و(85.71%) للموقع الثالث.